# AFFINE MOMENT INVARIANTS OF VECTOR FIELDS

*Jitka Kostková* ⋆ *Tomáš Suk*⋆ *Jan Flusser* ⋆

⋆ Czech Academy of Sciences
Institute of Information Theory and Automation
Pod vodárenskou věží 4, 182 08 Praha 8, Czech Republic

## ABSTRACT

Vector field (VF) is a special kind of multidimensional data. In each pixel, VF contains information about the direction and the magnitude of the measured quantity. To detect the patterns of interest in the field, special matching methods must be developed. We propose a method for the description and matching of VF patterns under an unknown affine transformation of the field. Unlike digital images, transformations of VFs act not only on the spatial coordinates but also on the field values, which makes the detection different. To measure the similarity between the template and the field patch, we propose original invariants with respect to affine transformation designed from moments. Their performance is demonstrated by experiments on real data from fluid mechanics.

***Index Terms***— Vector field, total transformation, affine invariants, template matching, vector field moments

## 1. INTRODUCTION

2D vector field $\mathbf{f}(\mathbf{x})$ can be mathematically described as a pair of scalar fields $\mathbf{f}(\mathbf{x}) = (f_1(\mathbf{x}), f_2(\mathbf{x}))$. At each point $\mathbf{x} = (x, y)$, the value of $\mathbf{f}(\mathbf{x})$ shows the orientation and the magnitude of the measured vector. Scalar field $f_i(\mathbf{x})$ can be understood as a graylevel image.

A common task in the vector field analysis is the detection of various patterns of interest. It comprises not only detection of singularities such as sinks, vortices and saddle points but also detection of patterns which are not specific but are similar to the pattern stored in the database. The detection of the patterns of interest is typically accomplished by *template matching*. The search algorithm must be primarily *invariant* with respect to all possible pattern deformations which might be present.

In this paper, we assume the template deformations can be modeled by so called *total affine transformation* (TAFT). We propose moment-based invariants w.r.t. TAFT, which can be efficiently used for template matching in vector fields.

This work was supported by the Czech Science Foundation (Grant No. GA18-07247S) and by the Grant Agency of the Czech Technical University (Grant No. SGS18/188/OHK4/3T/14). We thank Professor Mario Hlawitschka for providing the Kármán vortex street data.

## 2. VECTOR FIELDS AND THEIR TRANSFORMATIONS

By a total transformation we understand any transformation in the vector field space, which acts simultaneously in spatial and function domains. Even if this definition can be used for arbitrary (non-linear) transformations, in this paper we restrict to linear ones.

**Definition 1:** Let $A$ and $B$ be regular matrices and $\mathbf{f}$ be a vector field. The transformation $\mathbf{f} \to \mathbf{f}'$, where

$$\mathbf{f}'(\mathbf{x}) = B\mathbf{f}(A^{-1}\mathbf{x}) \tag{1}$$

is called *independent total affine transformation* of field $\mathbf{f}$. Matrix $A$ is called *inner* transformation matrix (or just inner transformation), while matrix $B$ is called *outer* transformation matrix.

In reality, vector fields are mostly transformed by a simpler transformation than (1) in which $A = B$. Such a model is called *special total affine transformation* and captures one of the basic properties of vector fields – if the field is transformed in the space domain, the function domain (i.e. the vector values) is transformed *by the same transformation*. This constitutes a significant difference from transformations of scalar images, where $B$ is usually the identity and only the inner transformation is effective.

## 3. LITERATURE SURVEY

Although affine invariants of vector fields have never been studied, there are still two categories of papers connected to our current work: papers on rotation invariants of vector fields and papers on affine invariants of scalar and color images.

The problem of finding vector field invariants to total rotation was raised for the first time by Schlemmer et al. [1]. Rotation invariants from geometric complex moments have found several applications. Liu and Ribeiro [2] used them to detect singularities on meteorological satellite images showing wind velocity and Liu and Yap [3] applied them to the indexing and recognition of fingerprint images. A generalization to more than two dimensions using tensor contraction was proposed by Langbein and Hagen [4]. Bujack et al.

[5] showed that the invariants can be derived also by means of the field normalization approach. Yang et al. improved the numerical stability of the invariants by using orthogonal Gaussian-Hermite [6] and Zernike [7] moments. Most recently, Bujack [8] introduced *flexible basis* of the invariants to avoid moments that vanish on the given templates. In all these papers, the authors considered the total rotation model only.

In contrast to the above group of papers on vector field rotation invariants, *affine moment invariants* (AMI) of graylevel images have been studied in hundreds of papers and books [9, 10, 11, 12, 13, 14]. Special AMIs were proposed for color images [15, 16, 17].

## 4. CONSTRUCTION OF VFAMI

In this section, we propose *vector field moment invariants w.r.t. total affine transformation* (VFAMI). The invariants are functions of geometric moments of the field. In case of 2D vector field $\mathbf{f}$ with components $f_1$ and $f_2$ we may use standard geometric scalar moments [18] given as

$$m_{pq}^{(i)} = \int_{-\infty}^{\infty}\int_{-\infty}^{\infty} x^p y^q f_i(x,y)\,\mathrm{d}x\,\mathrm{d}y\,. \qquad (2)$$

Let us for simplicity assume that $\mathbf{f}$ is compactly supported and both $f_i$ are piecewise continuous. Under these assumptions, all moments $m_{pq}^{(i)}$ of indices $p, q = 0, 1, 2, \ldots$ are well-defined and completely characterize field $\mathbf{f}$.

We need to achieve invariance w.r.t. both inner and outer transformation. First, to ensure the invariance to inner transform, we use the method proposed in [9] and further elaborated in [10].

Let us consider two arbitrary points $\mathbf{x}_i = (x_i, y_i)$, $i \in \{1, 2\}$, from the support of $\mathbf{f}$. Let us denote the "cross-product" of these points as $C_{12} = x_1 y_2 - x_2 y_1$. Geometric meaning of $C_{12}$ is the oriented double area of the triangle, whose vertices are $(x_1, y_1)$, $(x_2, y_2)$, and $(0, 0)$. After an affine transformation $\mathbf{x}' = A\mathbf{x}$ has been applied, the cross-product is transformed as $C'_{12} = J_A \cdot C_{12}$, where $J_A = \det(A)$ is the Jacobian of the transformation. This proves that $C_{12}$ is a relative invariant with respect to inner transformation $A$. Now we consider various numbers of points $(x_i, y_i)$ and we integrate their cross-products over the support of $\mathbf{f}$. These integrals can be expressed in terms of moments and, after eliminating the Jacobian by a proper normalization, they yield absolute affine invariants.

The invariance to outer transformation can be reached when using "component cross-products" $F_{kj}$ instead of $C_{kj}$

$$F_{kj} = f_1(x_k, y_k) f_2(x_j, y_j) - f_1(x_j, y_j) f_2(x_k, y_k)\,. \qquad (3)$$

$F_{kj}$ is a relative invariant w.r.t. outer affine transformation as $F'_{kj} = J_B \cdot F_{kj}$, where $J_B = \det(B)$.

The combination of both constructions stated above leads to the definition

$$V(\mathbf{f}) = \int_{-\infty}^{\infty}\cdots\int_{-\infty}^{\infty} \prod_{k,j=1}^{r} C_{kj}^{n_{kj}} \cdot F_{kj}^{v_{kj}} \cdot \prod_{i=1}^{r} \mathrm{d}x_i\,\mathrm{d}y_i\,. \qquad (4)$$

$V(\mathbf{f})$ is a relative invariant as

$$V(\mathbf{f}') = J_B^v J_A^w |J_A|^r V(\mathbf{f})\,, \qquad (5)$$

where $v = \sum v_{kj}$ and $w = \sum n_{kj}$. The number $w$ is called *weight* of the invariant and $2v$ is its *degree*.

To eliminate $J_A$ and $J_B$ and obtain an absolute invariant, we have to normalize the relative invariant (4) by proper powers of other two relative invariants such that both Jacobians get canceled. If $A = B$, the normalization factor consists of a single invariant only.

If used extensively with many various parameters, equation (4) yields a huge number of redundant invariants. The first step to eliminate the redundancy is that $V(\mathbf{f})$ must be composed solely of moments of field $\mathbf{f}$. Considering all possible index pairs $(k, j)$, each of the points $(x_1, y_1), \ldots, (x_r, y_r)$ must be involved just once in all $F_{kj}$'s used. Hence, any $v_{kj}$ can only equal 0 or 1, $v = r/2$ ($r$ must be even), and $v_{kj} = 0$ for all $k \geq j$ (this constraint is because $F_{kj} = -F_{jk}$ and $F_{kk} = 0$). If $v_{kj} = 1$, then $v_{mj} = v_{jm} = v_{km} = v_{mk} = 0$ for all index pairs different from $(k, j)$.

We may notice, that generating VFAMIs from Eq. (4), even if the choice of $v_{kj}$ has been constrained as mentioned above, leads to many invariants which are identically zero or which are somehow dependent on the other invariants that have been obtained from Eq. (4) with other settings of the parameters. Dependent invariants do not contribute to the recognition power of the system and only increase the dimensionality of the invariant set. It is highly desirable to identify them and exclude them from the set.

As an example, we show four simple VFAMIs in explicit forms below; hundreds of other invariants generated from Eq. (4) can be found on the web page [19].

The simplest non-trivial choice is $r = 2$ and $n_{12} = v_{12} = 1$, which yields

$$V_a = m_{10}^{(1)} m_{01}^{(2)} - m_{10}^{(2)} m_{01}^{(1)}\,.$$

The choice of $r = 2, v_{12} = 1$ and $n_{12} = 3$ yields

$$V_b = m_{30}^{(1)} m_{03}^{(2)} - 3m_{21}^{(1)} m_{12}^{(2)} + 3m_{12}^{(1)} m_{21}^{(2)} - m_{03}^{(1)} m_{30}^{(2)}\,.$$

The parameters $r = 2$, $v_{12} = 1$ and $n_{12} = 5$ lead to the invariant

$$\begin{aligned} V_c \;=\; & m_{50}^{(1)} m_{05}^{(2)} - 5m_{41}^{(1)} m_{14}^{(2)} + 10 m_{32}^{(1)} m_{23}^{(2)} \\ & -10 m_{23}^{(1)} m_{32}^{(2)} + 5 m_{14}^{(1)} m_{41}^{(2)} - m_{05}^{(1)} m_{50}^{(2)}\,. \end{aligned}$$

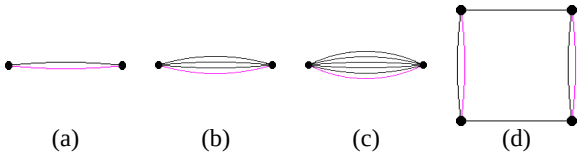


**Fig. 1**. The graphs representing invariants $V_a, V_b, V_c$ and $V_d$. The edges belonging to $E_1$ are shown in black, magenta edges belong to $E_2$.

If we choose $r = 4$, $v_{12}$ = $v_{34}$ = 1 and $n_{12}$=$n_{13}$=$n_{24}$=$n_{34}$=1, $n_{kj} = 0$ otherwise, we obtain

$$\begin{aligned} V_d &= -(m_{20}^{(1)})^2(m_{02}^{(2)})^2 + 4m_{20}^{(1)}m_{11}^{(1)}m_{11}^{(2)}m_{02}^{(2)} \\ &\quad +2m_{20}^{(1)}m_{02}^{(1)}m_{20}^{(2)}m_{02}^{(2)} - 4m_{20}^{(1)}m_{02}^{(1)}(m_{11}^{(2)})^2 \\ &\quad -4(m_{11}^{(1)})^2m_{20}^{(2)}m_{02}^{(2)} + 4m_{11}^{(1)}m_{02}^{(1)}m_{20}^{(2)}m_{11}^{(2)} - \\ &\quad (m_{02}^{(1)})^2(m_{20}^{(2)})^2 \,. \end{aligned}$$

## 5. VFAMI AND BI-LAYER GRAPHS

In this section, we establish the correspondence between VFAMIs generated by Eq. (4) and *bi-layer graphs*.

**Definition 2:** Let $\mathcal{V}$ be a set of vertices (nodes) and $E_1, E_2$ be sets of edges. $G = (\mathcal{V}; E_1, E_2)$ is called a *bi-layer graph* on $\mathcal{V}$. Graph $G_k = (\mathcal{V}; E_k)$ is called the *k-th layer* of graph $G$.

An arbitrary invariant generated by Eq. (4) can be represented by a bi-layer graph as follows. Each point $(x_k, y_k)$ corresponds to a graph node, so we have $r$ nodes. Each cross-product $C_{kj}$ corresponds to $n_{kj}$ edges of the first layer connecting the $k$th and $j$th nodes. The second layer is constructed in a similar way – each intensity cross-product $F_{kj}$ corresponds to $v_{kj}$ edges. In Fig. 1, we can see the graphs representing invariants $V_a, V_b, V_c$ and $V_d$ from Section 4.

We can immediately make several simple statements about the bi-layer graphs that represent VFAMIs from Eq. (4).

1. The number of nodes is even.
2. $G_1$ is a *multigraph*, it may contain multiple edges.
3. In $G_2$, all nodes have degree one. If $r > 2$, then $G_2$ is not a connected graph.
4. Neither layer is a directed graph.
5. Neither layer contains self-loops.
6. If $G$ is not connected, then the corresponding invariant is a product of several simpler invariants, which correspond to each connected component of $G$.
7. Any invariant of the form (4) is in fact a sum, where each term is a product of $r$ moments. The order of the moments is preserved in all terms. The moment orders contained in a single term are the same as the degrees of all vertices in $G_1$.

The proof of all above statements follows immediately from Eq. (4) and from the definition of the corresponding graphs. We can see that the problem of generating all invariants is equivalent to finding all connected bi-layer graphs, satisfying the constraints 1 – 5. An algorithm for a systematic generation of all such graphs can be found on the webpage [19].

## 6. NUMERICAL EXPERIMENTS

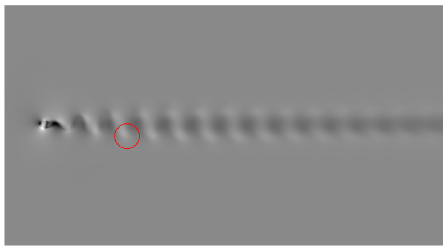

**Fig. 2**. The Kármán vortex street with the template selected for template matching.

In this experiment, we demonstrate the applicability of the proposed invariants in an important problem from fluid dynamics engineering – vortex detection in a fluid flow vector field. We used the field showing the Kármán vortex street, which is a repeating pattern of swirling vortices caused by the flow of a fluid around blunt bodies. In the Kármán pattern, we can see several vortices arranged into two rows. The orientation of the "street" is given by the main flow direction and is generally not known a priori.

A patch with a typical vortex is used as a template. In this task we used a vortex from the lower row (see Fig. 2), but generally, the template may be extracted from another similar field. To simulate this, we deformed the field (the template was not deformed) by special TAFT with $A = B$ which comprised anisotropic scaling with factors 5/4 and 7/4, respectively (the TAFT parameters were of course not revealed to the matching algorithm). The task is to find all vortices of a similar shape modulo TAFT. Hence, our aim is to find the lower row of vortices. The search is performed in the space of invariants $V_k$ up to the specified order/weight. We search for all local minima of $\ell_2$-distance below a user-defined threshold.

In Fig. 3, we can see the matching results in a single Kármán street frame for two different scaling factors. Almost all vortices, existing in the lower row, were detected successfully. The upper row was not detected, because the vortices are flipped comparing to the lower row (if desirable, this could be easily overcame by taking magnitudes of the invariants).

In order to perform an objective error analysis and to get statistical significance, we used a 300-frame video, showing the time-development simulation of the Kármán street. We used the same vortex template as before and matched it to

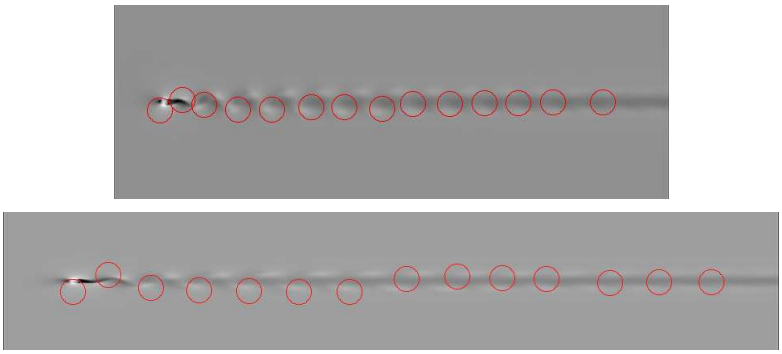

**Fig. 3**. Detected vortices by means of VFAMIs in the deformed fields (anisotropic scaling by 5/4 and 7/4 horizontally, respectively).

each frame individually. To avoid error propagation, no information from the previous frames was used. In each frame, the algorithm identified from 15 to 20 vortices, which are similar to the template. The videos with the vortex tracking for various scaling and choice of maximal weights are at [20].

To evaluate the accuracy, we measured the localization error of each vortex in each frame. The ground truth positions were deduced from the fluid mechanics theory, which guarantees (under ideal conditions) the equidistant placement of the vortices (this assumption, however, works approximately only in the first half of the street; the second half behaves differently and the ground-truth positions could not be estimated there).

We measured the absolute localization errors of all templates in the first half of each frame. We noticed there are two kinds of errors – *gross errors*, when the template localization error is greater than 10 pixels, and *small errors*, which are normally distributed errors in $x$ and $y$ not far from the ground-truth location. The absolute "small" localization errors in 2D follow Rayleigh distribution and we evaluate them by their mean. To evaluate the gross errors, we just counted false positives (FP), i.e. the templates that were found farther than 10 pixels from the expected position, and false negatives (FN), i.e. the cases when no template was found in the 10 pixel neighborhood of the expected position. The error statistics is summarized in Tables 1 and 2.

From these tables, we can make several conclusions. The first one is that the proposed invariants are actually able to detect templates in the VF which has undergone a TAFT. The second observation is that the number of both FP and FN is relatively high. This is caused by the choice of the neighborhood the invariants are calculated from. Since the TAFT parameters were considered unknown, the neighborhood was always a circle of the same size as the template. However, the actual neighborhood should be an ellipse (the circle deformed by matrix $A$). Since the invariants were calculated from non-corresponding patches, we obtained many mismatches. This also explains why the detection in the 5/4 case was detected better than in the 7/4 case and why the invariants of weight 6 and 7 do not improve the accuracy in the latter case. In this simulated case we could took the exact ellipses and improve the accuracy a lot but this would be unrealistic in practice and unfair.

| max. weight | # matches | FN | FP | mean |
|---|---|---|---|---|
| 3 | 1748 | 343 | 291 | 6.673 |
| 4 | 1823 | 109 | 132 | 5.775 |
| 5 | 2030 | 81 | 311 | 4.002 |
| 6 | 1840 | 96 | 136 | 3.859 |
| 7 | 2082 | 82 | 364 | 3.816 |

**Table 1**. Matching statistics on the scale 5/4.

| max. weight | # matches | FN | FP | mean |
|---|---|---|---|---|
| 3 | 1688 | 1800 | 1688 | – |
| 4 | 1870 | 454 | 524 | 4.107 |
| 5 | 1929 | 266 | 395 | 4.055 |
| 6 | 2053 | 381 | 634 | 4.171 |
| 7 | 2268 | 319 | 787 | 4.114 |

**Table 2**. Matching statistics on the scale 7/4.

## 7. CONCLUSION

This paper introduced invariants of vector fields w.r.t. total affine transformation based on the moments of the vector field. The behavior of VFs under TAFT is significantly different from scalar and color images under affine transformation and the traditional techniques cannot be used. We demonstrated the performance of the invariants on template matching on the real data from fluid dynamics. However, the choice of the neighborhood the invariants are calculated from is still an open problem.

## 8. REFERENCES


[1] Michael Schlemmer, Manuel Heringer, Florian Morr, Ingrid Hotz, Martin-Hering Bertram, Christoph Garth, Wolfgang Kollmann, Bernd Hamann, and Hans Hagen, "Moment invariants for the analysis of 2D flow fields," *IEEE Transactions on Visualization and Computer Graphics*, vol. 13, no. 6, pp. 1743–1750, 2007.

[2] Wei Liu and Eraldo Ribeiro, "Detecting singular patterns in 2-D vector fields using weighted Laurent polynomial," *Pattern Recognition*, vol. 45, no. 11, pp. 3912–3925, 2012.

[3] Manhua Liu and Pew-Thian Yap, "Invariant representation of orientation fields for fingerprint indexing," *Pattern Recognition*, vol. 45, no. 7, pp. 2532–2542, 2012.

[4] Max Langbein and Hans Hagen, "A generalization of moment invariants on 2D vector fields to tensor fields of arbitrary order and dimension," in *Proceedings of 5th International Symposium Advances in Visual Computing, ISVC'09, Part II*. 2009, vol. 5876 of *Lecture Notes in Computer Science*, pp. 1151–1160, Springer.

[5] Roxana Bujack, Mario Hlawitschka, Gerik Scheuermann, and Eckhard Hitzer, "Customized TRS invariants for 2D vector fields via moment normalization," *Pattern Recognition Letters*, vol. 46, no. 1, pp. 46–59, 2014.

[6] Bo Yang, Jitka Kostková, Tomáš Suk, Jan Flusser, and Roxana Bujack, "Recognition of patterns in vector fields by Gaussian–Hermite invariants," in *International Conference on Image Processing ICIP'17*, Jiebo Luo, Wenjun Zeng, and Yu-Jin Zhang, Eds. 2017, pp. 2350–2363, IEEE.

[7] Bo Yang, Jitka Kostková, Jan Flusser, Tomáš Suk, and Roxana Bujack, "Rotation invariants of vector fields from orthogonal moments," *Pattern Recognition*, vol. 74, pp. 110–121, 2017.

[8] Roxana Bujack and Jan Flusser, "Flexible basis of rotation moment invariants," in *International Conferences in Central Europe on Computer Graphics, Visualization and Computer Vision WSCG'17*, Václav Skala, Ed., 2017.

[9] Tomáš Suk and Jan Flusser, "Graph method for generating affine moment invariants," in *Proceedings of the 17th International Conference on Pattern Recognition ICPR'04*. 2004, pp. 192–195, IEEE Computer Society.

[10] Tomáš Suk and Jan Flusser, "Affine moment invariants generated by graph method," *Pattern Recognition*, vol. 44, no. 9, pp. 2047–2056, 2011.

[11] Thomas H. Reiss, *Recognizing Planar Objects Using Invariant Image Features*, vol. 676 of *LNCS*, Springer, Berlin, Germany, 1993.

[12] Tomáš Suk and Jan Flusser, "Affine moment invariants generated by automated solution of the equations," in *Proceedings of the 19th International Conference on Pattern Recognition ICPR'08*. 2008, IEEE Computer Society.

[13] Mark S. Hickman, "Geometric moments and their invariants," *Journal of Mathematical Imaging and Vision*, vol. 44, no. 3, pp. 223–235, 2012.

[14] I. Rothe, H. Süsse, and K. Voss, "The method of normalization to determine invariants," *IEEE Transactions on Pattern Analysis and Machine Intelligence*, vol. 18, no. 4, pp. 366–376, 1996.

[15] Tomáš Suk and Jan Flusser, "Affine moment invariants of color images," in *Computer Analysis of Images and Patterns CAIP'09*, Xiaoyi Jiang and Nikolai Petkov, Eds. September 2009, vol. LNCS 5702, pp. 334–341, Springer.

[16] Florica Mindru, Tinne Tuytelaars, Luc Van Gool, and Theo Moons, "Moment invariants for recognition under changing viewpoint and illumination," *Computer Vision and Image Understanding*, vol. 94, no. 1–3, pp. 3–27, 2004.

[17] Ming Gong, You Hao, Hanlin Mo, and Hua Li, "Naturally combined shape-color moment invariants under affine transformations," *Computer Vision and Image Understanding*, vol. 162, pp. 46–56, 2017.

[18] Jan Flusser, Tomáš Suk, and Barbara Zitová, *2D and 3D Image Analysis by Moments*, Wiley, Chichester, U.K., 2016.

[19] Jan Flusser and Tomáš Suk, "Affine moment invariants of vector fields," 2018, `http://zoi.utia.cas.cz/affine-vector-fields`.

[20] Jitka Kostková, Jan Flusser, and Tomáš Suk, "Experiment with Kármán street," 2018, `http://zoi.utia.cas.cz/Experiment-with-Karman-Street`.